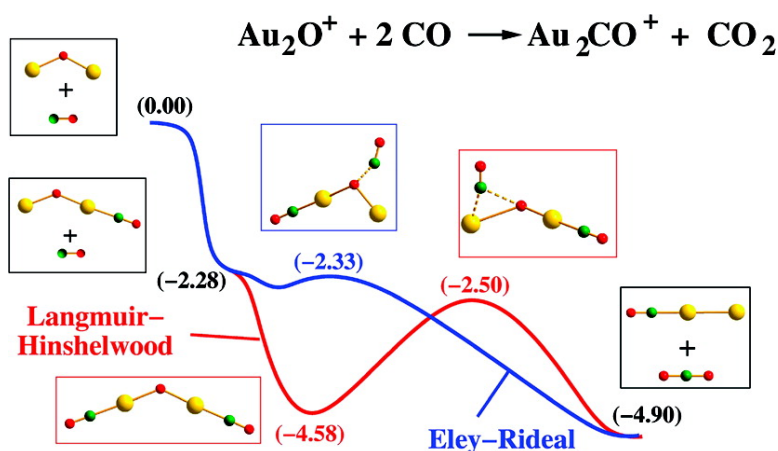


Influence of Charge State on the Mechanism of CO Oxidation on Gold Clusters

Christian Brgel, Nelly M. Reilly, Grant E. Johnson, Roland Mitri,
 Michele L. Kimble, A. W. Castleman, and Vlasta Bonacchi-Koutecký

J. Am. Chem. Soc., **2008**, 130 (5), 1694-1698 • DOI: 10.1021/ja0768542

Downloaded from <http://pubs.acs.org> on February 8, 2009



More About This Article

Additional resources and features associated with this article are available within the HTML version:

- Supporting Information
- Links to the 3 articles that cite this article, as of the time of this article download
- Access to high resolution figures
- Links to articles and content related to this article
- Copyright permission to reproduce figures and/or text from this article

[View the Full Text HTML](#)

Influence of Charge State on the Mechanism of CO Oxidation on Gold Clusters

Christian Bürgel,[†] Nelly M. Reilly,[‡] Grant E. Johnson,[‡] Roland Mitrić,[†]
Michele L. Kimble,[‡] A. W. Castleman, Jr.,^{*,‡} and Vlasta Bonačić-Koutecký^{*,†}

Institut für Chemie, Humboldt Universität zu Berlin, Brook-Taylor-Strasse 2, 12489 Berlin, Germany, and Departments of Chemistry and Physics, The Pennsylvania State University, University Park, Pennsylvania 16802

Received September 10, 2007; E-mail: awc@psu.edu

Abstract: We present results from our joint experimental and theoretical study of the reactivity of anionic and cationic gold oxide clusters toward CO, focusing on the role of atomic oxygen, different charge states, and mechanisms for oxidation. We show that anionic clusters react by an Eley–Rideal-like mechanism involving the preferential attack of CO on oxygen rather than gold. In contrast, the oxidation of CO on cationic gold oxide clusters can occur by both an Eley–Rideal-like and a Langmuir–Hinshelwood-like mechanism at multiple collision conditions as a result of the high adsorption energy of two CO molecules. This large energy of CO adsorption on cationic gold oxide clusters is the driving force for the CO oxidation. Therefore, in the presence of cationic gold species at high pressures of CO, the oxidation reaction is self-promoting (i.e., the oxidation of one CO molecule is promoted by the binding of a second CO). Our findings provide new insight into the role of charge state in gold-cluster-based nanocatalysis.

1. Introduction

The oxidation of CO in the presence of gold has drawn considerable attention due to the findings of Haruta and co-workers.^{1–4} The discovery that small gold particles are efficient in promoting oxidation reactions has prompted many condensed- and gas-phase experimental and theoretical studies.^{5,6} However, there are still open questions regarding size, charge state and support effects, the nature of the active site, as well as the responsible mechanisms which remain to be answered. So far, the focus has largely been on weakening the molecular oxygen bond as a possible mechanism to promote the oxidation reaction. The general view is that neutral gold clusters alone cannot activate the O–O bond without influences from the substrate such as a charge-transfer process.⁷ Previous studies have demonstrated that F-center defects present on MgO surfaces transfer charge to the supported gold clusters. This charge then occupies the $2\pi^*$ orbital of O₂ which weakens the O–O bond.⁸ More recent work,^{9–11} however, has demonstrated that charging

of adsorbed metals does not always involve the presence of defects on the oxide surface. Both experimental and theoretical studies have verified the presence of charged gold species on thin defect-free MgO surfaces supported on Mo and Ag.^{9–11} It is proposed that by varying the thickness of the MgO layer, and thereby the work function of the underlying metal, it may be possible to tune the charging of the supported Au clusters.¹⁰

Recent literature shows that gold oxides containing both atomic and molecular oxygen may play a role as the active site in supported gold catalysts.^{12–14} In fact, it has been shown through TOF–SIMS that AuO[−] is a structural feature found on supported gold clusters.¹⁴ Recent studies have also identified the presence of cationic gold centers in operational supported gold catalysts for CO oxidation.¹⁵ Through a variety of analytical techniques, it was recently confirmed that for gold catalysts supported on Fe₂O₃, gold is present in both the metallic and cationic forms and that cationic gold is essential for high CO oxidation efficiency.¹⁵ Other studies have shown that the cationic gold initially present in the working catalyst is reduced to metallic gold through exposure to CO, which thereby lowers the catalytic activity through poisoning.¹⁶ Therefore, a fundamental question can be raised as to the influence of the charge state and the binding of multiple CO molecules on the reactivity of gold oxides containing atomic and molecular oxygen. In

[†] Humboldt Universität zu Berlin.

[‡] The Pennsylvania State University.

- (1) Haruta, M. *Catal. Today* **1997**, *36*, 153–166.
- (2) Haruta, M.; Yamada, N.; Kobayashi, T.; Iijima, S. *J. Catal.* **1989**, *115*, 301–309.
- (3) Haruta, M.; Tsubota, S.; Kobayashi, T.; Kageyama, H.; Genet, M. J.; Delmon, B. *J. Catal.* **1993**, *144*, 175–192.
- (4) Daté, M.; Haruta, M. *J. Catal.* **2001**, *201*, 221–224.
- (5) Bond, G. C.; Thompson, D. T. *Catal. Rev.—Sci. Eng.* **1999**, *41*, 319–388.
- (6) Bernhardt, T. M. *Int. J. Mass Spectrom.* **2005**, *243*, 1–29.
- (7) Sanchez, A.; Abbet, S.; Heiz, U.; Schneider, W. D.; Häkkinen, H.; Barnett, R. N.; Landman, U. *J. Phys. Chem. A* **1999**, *103*, 9573–9578.
- (8) Yoon, B.; Häkkinen, H.; Landman, U.; Worz, A. S.; Antonietti, J. M.; Abbet, S.; Judai, K.; Heiz, U. *Science* **2005**, *307*, 403–407.
- (9) Zhang, C.; Yoon, B.; Landman, U. *J. Am. Chem. Soc.* **2007**, *129*, 2228–2229.
- (10) Sterrer, M.; Risse, T.; Pozzoni, U.; Giordano, L.; Heyde, M.; Rust, H.; Pacchioni, G.; Freund, H. *Phys. Rev. Lett.* **2007**, *98*, 096107.

- (11) Honkala, K.; Häkkinen, H. *J. Phys. Chem. C* **2007**, *111*, 4319–4327.
- (12) Oh, H. S.; Costello, C. K.; Cheung, C.; Kung, H. H.; Kung, M. C. *Stud. Surf. Sci. Catal.* **2001**, *139*, 375–381.
- (13) Kung, H. H.; Kung, M. C.; Costello, C. K. *J. Catal.* **2003**, *216*, 425–432.
- (14) Fu, L.; Wu, N. Q.; Yang, J. H.; Qu, F.; Johnson, D. L.; Kung, M. C.; Kung, H. H.; Dravid, V. V. *J. Phys. Chem. B* **2005**, *109*, 3704–3706.
- (15) Hutchings, G.; Hall, M.; Carley, A.; Landon, P.; Solsona, B.; Kiely, C.; Herzing, A.; Makkee, M.; Moulijn, J.; Overweg, A.; Fierro-Gonzales, J.; Guzman, J.; Gates, B. *J. Catal.* **2006**, *242*, 71–81.
- (16) Guzman, J.; Gates, B. *J. Am. Chem. Soc.* **2004**, *126*, 2672–2673.

particular, a different charge state (anionic vs cationic) can lead to a preference for an Eley–Rideal¹⁷ (ER)- or a Langmuir–Hinshelwood¹⁷ (LH)-type mechanism for CO oxidation.

In the ER mechanism, a CO molecule from the gas phase directly attacks the oxygen atom bound to the gold cluster, and subsequently, CO₂ is formed. In contrast, in the LH mechanism, the CO molecule is first bound to a gold atom, and subsequently, either the system can rearrange or the adsorbed CO can directly attack the surrounding oxygen centers (intrasystem attack). Since, in general, CO binds strongly to all cationic clusters,¹⁸ in contrast to anionic clusters which show pronounced size dependence of the CO binding energy,¹⁹ it is expected that a preference for one of these mechanisms will be strongly dependent on the charge state of the gold cluster.

The goal of our joint experimental and theoretical study is to provide fundamental insight into the mechanism of CO oxidation in the presence of mass-selected anionic and cationic gold oxide clusters. A crucial aspect of the present experimental study is the production of species containing atomic oxygen, enabling investigation of the influence of dissociated oxygen on the reactions of CO in the presence of anionic and cationic gold. Furthermore, theoretical exploration allows for the determination of energetics along the reaction pathways as well as the proposal of viable general mechanisms, which are confirmed by ab initio energetics and molecular dynamics simulations.

In the case of anionic gold oxide clusters, we showed in a previous publication that a peripheral O atom is the most effective center for the oxidation reaction which occurs on anionic AuO⁻ and Au₂O⁻ species.¹⁹ However, this previous study also revealed that the presence of a peripheral oxygen is not always sufficient for the oxidation reaction to proceed (e.g., in the case of Au₃O₂⁻).¹⁹ In this publication, we show that, due to the generally low binding energy of CO to anionic gold clusters, the oxidation reaction proceeds according to an ER-like mechanism. In switching from anionic to cationic clusters, the influence of the CO binding energy becomes evident. Consequently, the presence of atomic (peripheral and bridging) oxygen is not alone sufficient to allow the oxidation reaction to proceed. In fact, in the case of cationic gold clusters, we demonstrate here that the oxidation reaction occurs under multiple collision conditions and is driven by a large energy gain upon adsorption of two CO molecules. In this case, both ER- and LH-like mechanisms become generally favorable and lead to the oxidation of CO. Thus, our results indicate that small cationic gold centers might be the most effective sites for CO oxidation. For larger size clusters, adsorption of multiple CO molecules may lead to cluster fragmentation, producing small active units. Alternatively, the CO may bind to a site which is further away from the reaction center and, therefore, will not be efficiently oxidized. This demonstrates that, in addition to structure and size selectivity aspects, the charge state of gold species has a significant influence on the oxidation reaction mechanism (ER vs LH).

2. Experimental Methods

The experimental studies were carried out for gold oxides with both atomized and molecular oxygen utilizing a guided ion beam (GIB)

apparatus described in detail elsewhere.²⁰ Briefly, gold oxide clusters were produced in a laser vaporization cluster source by pulsing oxygen seeded in helium (20% for cations and 80% for anions) into the plasma formed by ablating a rotating and translating gold rod with the second harmonic (532 nm) of a Nd:YAG laser. The clusters exit the source region through a 51 mm conical nozzle and are cooled through supersonic expansion into vacuum. The clusters pass through a 3 mm skimmer forming a collimated molecular beam and are directed into the first quadrupole mass filter employing a set of electrostatic lenses. The first quadrupole mass filter isolates clusters of a desired stoichiometry which are then directed into an octopole collision cell using a second set of electrostatic lenses. Variable pressures of CO are introduced into the octopole collision cell employing a low flow leak valve. The CO pressure is monitored using a MKS Baratron capacitance manometer attached to the collision cell. The product ions formed in the collision cell are extracted with a third set of electrostatic lenses and mass analyzed by a second quadrupole mass spectrometer. Finally, the ions are detected with a channeltron electron multiplier connected to a multichannel scalar card housed in a personal computer. The kinetic energy imparted to the cluster ions by the supersonic expansion was experimentally determined, by employing a retarding potential analysis,²⁰ to be around 0.1 eV in the center-of-mass energy frame. The entrance lens to the octopole collision cell was maintained at a potential of 0 V to ensure that no additional energy was imparted to the clusters by the first two sets of focusing lenses. The GIB mass spectrometer allowed for mass-selected species to undergo reactions with CO. The experimental branching ratios presented in the Results section illustrate the change in normalized ion intensity with increasing pressures of CO reactant gas. At higher gas pressures, therefore, the ratio of reactant ion intensity to total ion intensity becomes smaller, while the ratio of product ion intensity to total ion intensity becomes larger. Some attenuation of ion signal does occur at higher reactant gas pressures, and it is assumed that both the reactant and product ion intensities are reduced equally. The same GIB apparatus was employed to confirm the results from previous flow tube studies for the anionic clusters¹⁹ and to investigate the reactivity of cationic gold oxides with CO. The presence of atomic versus molecular oxygen was confirmed via collisional studies in the guided ion beam mass spectrometer.¹⁹ In these experiments, the gold oxides produced in the laser vaporization source were subjected to the same pressure of inert nitrogen in the octopole as that of CO. The resulting fragments verified structural features, such as the existence of molecular or atomized oxygen, and confirmed that the oxygen loss products observed with CO were the result of chemical reactions and not the products of collisional fragmentation.

3. Theoretical Calculations

Geometrical properties and the reactivity of the gold oxide anionic and cationic clusters were studied using a DFT method with the B3LYP functional.^{21–23} Relativistic effects which are strongly pronounced in the case of gold were taken into account by using the 19-electron relativistic effective core potential (19-RECP) from the Stuttgart group and the (8s7p5d1f)/[7s5p3d1f] atomic orbital (AO) basis set.^{24,25} For the oxygen and carbon atoms, the triple-split valence basis set 6-311G-(d) was employed. Our previous theoretical work on the adsorption of O₂ onto hydrated gold clusters²⁶ and the oxidation of CO by gold anions^{19,27} has shown that DFT provides the appropriate accuracy needed for determination of binding energies and energetics. This was checked

(17) Ertl, G. *Surf. Sci.* **1994**, *299*, 742–754.

(18) Neumaier, M.; Weigend, F.; Hampe, O.; Kappes, M. M. *J. Chem. Phys.* **2005**, *122*, 104702.

(19) Kimble, M. L.; Moore, N. A.; Johnson, G. E.; Castleman, A. W., Jr.; Bürgel, C.; Mitrić, R.; Bonačić-Koutecký, V. *J. Chem. Phys.* **2006**, *125*, 204311.

(20) Bell, R. C.; Zemski, K. A.; Justes, D. R.; Castleman, A. W., Jr. *J. Chem. Phys.* **2001**, *114*, 798–811.

(21) Becke, A. D. *Phys. Rev. A* **1998**, *38*, 3098–3100.

(22) Becke, A. D. *J. Chem. Phys.* **1993**, *98*, 5648–5652.

(23) Lee, C.; Yang, W.; Parr, R. G. *Phys. Rev. B* **1998**, *37*, 785–789.

(24) Andrae, D.; Haeussermann, U.; Dolg, M.; Stoll, H.; Preuss, H. *Theor. Chim. Acta* **1990**, *77*, 123–141.

(25) Gilb, S.; Weis, P.; Furche, F.; Ahlrichs, R.; Kappes, M. M. *J. Chem. Phys.* **2002**, *116*, 4094–4101.

(26) Wallace, W. T.; Wyrwas, R. B.; Whetten, R. L.; Mitrić, R.; Bonačić-Koutecký, V. *J. Am. Chem. Soc.* **2003**, *125*, 8408–8414.

by comparison with coupled cluster [CCSD(T)] calculations based on highly correlated wave functions. The energy sequences as well as the binding energies are generally not altered in the more accurate calculations. Moreover, the MRD-CI method was used to check that there was no multireference nature of the wave function along the reaction pathways. However, a systematic investigation of the influence of suitable basis sets for highly correlated wave functions is needed for high precision which is beyond the scope of this work.

All structures presented here are fully optimized using gradient minimization techniques, and stationary points have been characterized as minima or transition states by calculating the frequencies. Moreover, the reaction mechanisms have been determined by calculating the energy profiles based on electronic energies of the DFT calculations, which correspond to the microcanonical conditions at low pressure in the GIB experiments presented here.

The reaction mechanisms were also revealed by performing ab initio molecular dynamics (MD) simulations “on the fly” based on the DFT method. In order to improve efficiency, the resolution of identity (RI)-DFT procedure^{28,29} has been employed involving the Perdew–Burke–Ernzerhof (PBE³⁰) functional with the 19-electron relativistic effective core pseudopotential (19e-RECPs) for gold combined with Gaussian basis sets of triple- ζ quality for all atoms.²⁴

4. Results and Discussion

In order to determine the influence of charge state on the oxidation of CO, we studied the reactions of AuO^\pm and Au_2O^\pm in detail. As presented in Figure 1, the branching ratios show that an oxidation reaction occurs for anionic AuO^- and Au_2O^- . This is evident from a decrease in the intensity of these species with CO addition, while the intensity of Au^- and Au_2^- , which are O atom loss products, increases with higher CO pressure. Formation of Au^- and Au_2^- was not observed in experiments employing N_2 gas, indicating that these species are the result of a chemical reaction with CO and not the products of collisional dissociation of an O atom from AuO^- and Au_2O^- . In the case of AuO^- and Au_2O^- , the peripheral oxygen atom is the reactive center which is responsible for the CO oxidation that occurs via a charge-transfer mechanism. The snapshots in Figure 2 demonstrate the occurrence of the oxidation reaction which proceeds according to an ER-type mechanism. These oxidation reactions follow a general mechanism which involves formation of a complex with a weakly bound CO molecule.¹⁹ This is followed by transfer of the unpaired electron from the O^- atom to the π^* orbital of CO, giving rise to the formation of a complex with a CO_2^- subunit according to the calculated net spin density based on the Mulliken population analysis. The final emanation of CO_2 is accompanied by an electron transfer from the CO_2 subunit back to gold as evidenced by the natural bonding orbital (NBO³¹) charge analysis. This reaction mechanism is valid for the oxidation reactions found for anionic monomer and dimer oxides with a peripheral oxygen atom (AuO_3^- , Au_2O_3^- , and Au_2O_4^-).¹⁹

For the oxidation reaction to proceed according to a LH mechanism, two requirements have to be fulfilled. First, the CO

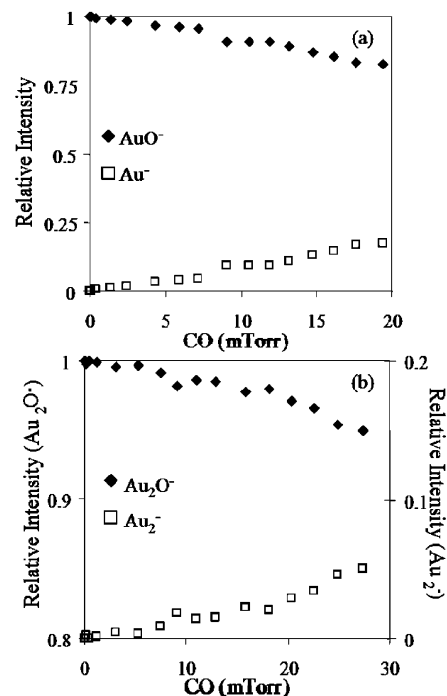


Figure 1. Branching ratio for the reaction of (a) AuO^- and (b) Au_2O^- with CO. Notice the decrease in the selected parent ion signal and the concomitant increase in the O atom loss product species, Au^- and Au_2^- , respectively. The initial kinetic energy of the ions is approximately 0.1 eV in the center-of-mass energy frame.

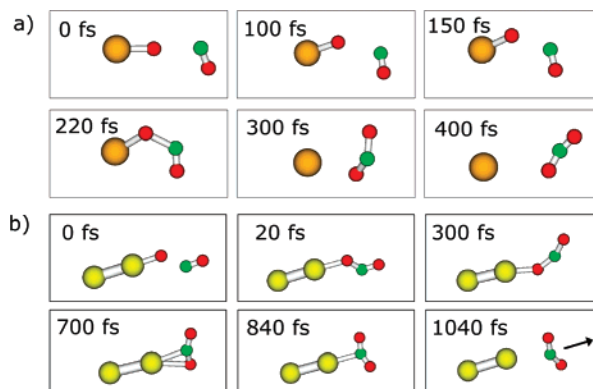


Figure 2. MD snapshots for the reaction of (a) AuO^- and (b) Au_2O^- with CO. Both species show CO reacting with a peripheral oxygen atom on the gold oxide cluster to produce CO_2 by the ER mechanism.

binding energy has to be sufficiently large, and second, the barriers for subsequent O–C bond formation have to be lower than the energy gained during the CO adsorption. In the case of AuO^- and Au_2O^- , the calculated binding energies of CO to a gold atom are 2.3 and 0.4 eV, respectively. However, the barrier for the subsequent rearrangement in which the carbon atom migrates from the gold site and attacks the oxygen atom is higher than 2 eV, making the LH mechanism for the oxidation reaction difficult for AuO^- and unfeasible for Au_2O^- .

In contrast, by changing the charge state, the branching ratios in Figure 3 for AuO^+ and Au_2O^+ show that the dominant reaction channel is apparently loss of a single O atom and the association of a CO molecule. However, this process is calculated to be only moderately exothermic by 0.63 eV for AuO^+ and endothermic by 0.81 eV for Au_2O^+ . Therefore, the loss of atomic O and the association of CO cannot explain the

(27) Kimble, M. L.; Castleman, A. W., Jr.; Mitrić, R.; Bürgel, C.; Bonačić-Koutecký, V. *J. Am. Chem. Soc.* **2004**, *126*, 2526–2535.

(28) Dunlap, B. I.; Connolly, J. W. D.; Sabin, J. R. *J. Chem. Phys.* **1979**, *71*, 3396–3402.

(29) Eichkorn, K.; Treutler, O.; Öhm, H.; Häser, M.; Ahlrichs, R. *Chem. Phys. Lett.* **1995**, *242*, 652–660.

(30) Perdew, J. P.; Burke, K.; Ernzerhof, M. *Phys. Rev. Lett.* **1996**, *77*, 3865–3868.

(31) Reed, A. E.; Weinhold, F.; Curtiss, L. A.; Pochatko, D. J. *J. Chem. Phys.* **1986**, *84*, 5687–5705.

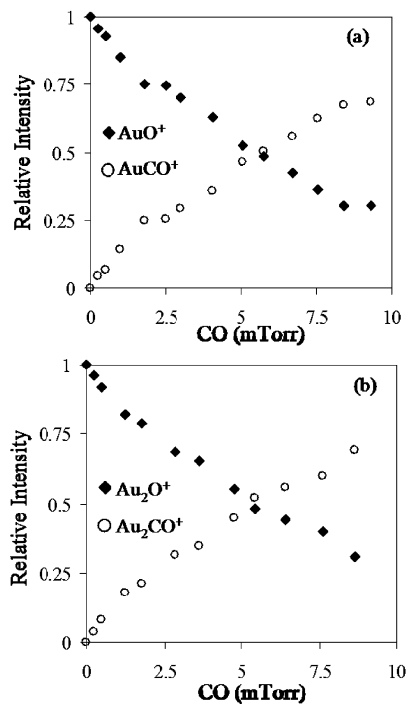


Figure 3. Branching ratios for the reaction of (a) AuO^+ and (b) Au_2O^+ with CO. Notice the decrease in the selected parent ion signal and the concomitant increase in oxygen atom replacement by CO. The initial kinetic energy of the ions is approximately 0.1 eV in the center-of-mass energy frame.

experimental branching ratios shown in Figure 3 for Au_2O^+ and is also unlikely for AuO^+ . Moreover, carbide formation by CO cleavage and subsequent loss of an O atom ($\text{AuO}^+ + \text{CO} \rightarrow \text{O}-\text{Au}-\text{C}^+ + \text{O}$) can be excluded since it is energetically highly unfavorable (endothermic by >8 eV; barrier for breaking the C–O bond >6.8 eV). Since the experiments were carried out under multiple collision conditions, an oxidation reaction involving two CO molecules according to the formula $\text{Au}_{1,2}\text{O}^+ + 2\text{CO} \rightarrow \text{Au}_{1,2}\text{CO}^+ + \text{CO}_2$ is possible and leads to the same products as those observed in the experiments. Moreover, these reaction channels are calculated to be thermodynamically favorable both for AuO^+ (-3.25 eV) and Au_2O^+ (-4.90 eV). The profiles for the oxidation reactions involving two CO molecules are presented in Figure 4. In the case of AuO^+ (Figure 4a), the adsorption of the first CO molecule leads to the formation of a complex which is 2.26 eV more stable than the reactants. From this point, the reaction with the second CO molecule can occur either by an ER- or LH-type mechanism. According to the ER mechanism, the second CO molecule from the gas phase reacts directly with the peripheral O atom, leading to the formation of the experimentally observed products without significant barriers. The LH mechanism involves the initial binding of CO to the gold atom (leading to $\text{O}-\text{Au}-\text{CO}^+$) followed by an internal attack on the peripheral O atom, involving a barrier of about 1.73 eV. Subsequently, the CO_2 is released, and the second CO adsorbs to the Au^+ ion, giving rise to the observed final product. However, due to the energetics, the oxidation according to a LH mechanism is less favorable than the ER mechanism for AuO^+ . A third pathway involving binding of the second CO to the gold atom in $\text{O}-\text{Au}-\text{CO}^+$ causes fragmentation of the O atom leading to $\text{Au}(\text{CO})_2^+$ which is not observed experimentally.

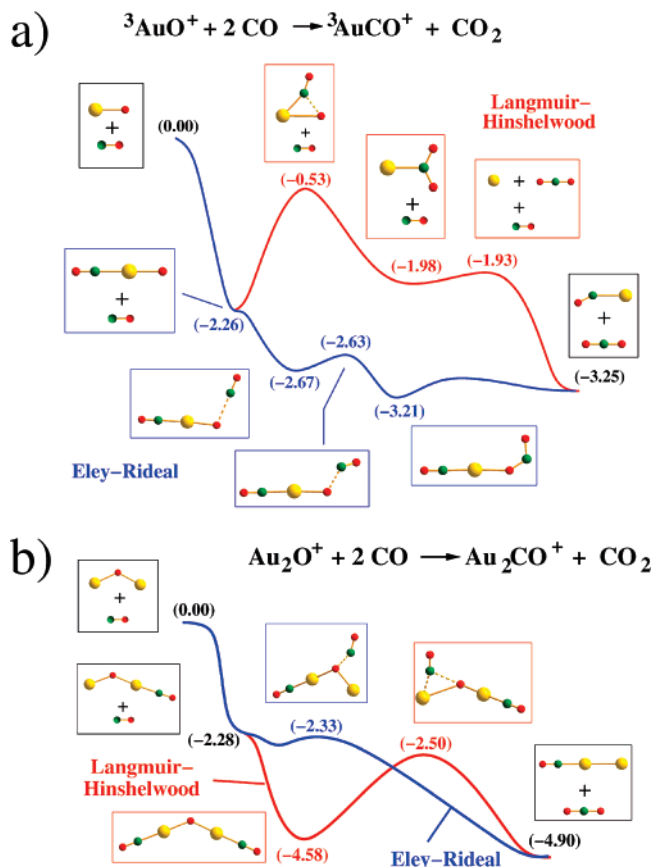


Figure 4. Energy profiles for the reaction of CO with (a) AuO^+ and (b) Au_2O^+ . All energies are given in electron volts (eV) relative to the energy of the reactants ($\text{Au}_{1,2}\text{O}^+ + 2\text{CO}$) at 0 K. Shown are ER-like (blue) and LH-like (red) mechanisms. For the reaction of Au_2O^+ with CO according to the ER-like mechanism, a barrier of ~ 0.2 eV and an excess energy of ~ 2.5 eV have been calculated for the rate-determining step. For the LH-like mechanism, the calculated barrier and excess energy are 2.08 and 4.58 eV, respectively.

In the case of Au_2O^+ (Figure 4b), adsorption of the first CO molecule yields a complex which is more stable than the reactants by 2.28 eV. Similar to AuO^+ , the oxidation of a second CO molecule can easily occur according to the ER-like mechanism since the involved small barriers (~ 0.2 eV³²) can be easily overcome as depicted in Figure 4b. However, Au_2OCO^+ can directly bind a second CO molecule due to a free Au adsorption site. Notice that this is not the case for $\text{O}-\text{Au}-\text{CO}^+$ because the binding of a second CO disrupts the strongly favored linear coordination of the atomic gold center and thus leads to the already mentioned loss of the weakly bound O atom. In contrast, the binding of the second CO onto $\text{Au}_2\text{O}(\text{CO})^+$ provides additional energy of 2.30 eV. Therefore, the overall energy gain of 4.58 eV is sufficient to overcome the barrier (2.08 eV) for the attack of a bound CO molecule on the bridging O atom according to the LH mechanism. Therefore, both ER- and LH-like mechanisms are viable for CO oxidation on Au_2O^+ . These findings are further supported by our MD simulations presented in Figure 5, which show that the reaction can proceed according to both types of mechanisms. However, in agreement with simple modeling of the relative rate constants according

(32) The weakly bound complex between $\text{O}-\text{Au}-\text{CO}^+$ and the second CO has not been fully optimized and is therefore not shown in Figure 4. The relative energy with respect to the reactants is about -2.5 eV.

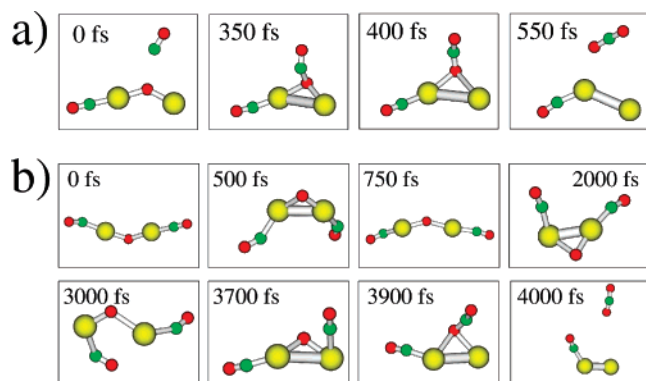


Figure 5. MD snapshots for the reaction $\text{Au}_2\text{O}^+ + 2\text{CO} \rightarrow \text{Au}_2\text{CO}^+ + \text{CO}_2$ according to (a) the ER-like mechanism and (b) the LH-like mechanism.

to the Rice–Ramsperger–Kassel (RRK) theory, the LH process would occur considerably more slowly.

5. Conclusion

Our joint gas-phase experimental and theoretical studies presented herein provide new insights into the influence of charge state on the mechanism of CO oxidation. We show that

anionic clusters react by an Eley–Rideal-like mechanism involving the preferential attack of CO on oxygen rather than gold. In contrast, the oxidation of CO on cationic gold oxide clusters can occur by both an Eley–Rideal-like and a Langmuir–Hinshelwood-like mechanism at multiple collision conditions as a result of the high adsorption energy of two CO molecules. This large energy of CO adsorption on cationic gold oxide clusters is the driving force for CO oxidation in the gas phase where the energy is completely retained by the clusters. Therefore, in the presence of cationic gold species at high pressures of CO, the oxidation reaction is self-promoting (i.e., the oxidation of one CO molecule is promoted by the binding of a second CO). Our findings provide new insight into the role of charge state in gold-cluster-based nanocatalysis.

Acknowledgment. N.M.R., G.E.J., M.L.K., and A.W.C. gratefully acknowledge the Department of Energy, Grant Number DE-FG02-92ER14258, for their financial support. C.B., R.M., and V.B.K. acknowledge the Deutsche Forschungsgemeinschaft. G.E.J. gratefully acknowledges Eric Tyo for helpful discussions.

JA0768542